J. Fluid Mech. (1976), *vol.* 76, *part* 3, *pp.* 417–432
Printed in Great Britain

Viscous eddies near a 90° and a 45° corner in flow through a curved tube of triangular cross-section

By W. M. COLLINS AND S. C. R. DENNIS

Department of Applied Mathematics, University of Western Ontario, London, Canada

(Received 14 August 1975 and in revised form 17 May 1976)

A numerical calculation is presented for the slow flow of a viscous fluid in a region bounded by a right-angled isosceles triangle. The particular flow considered is the secondary flow generated in the plane of a cross-section by the primary axial flow, under a constant pressure gradient, through a slightly curved tube of triangular cross-section. The flow is assumed to be at small Dean number so that the stream function of the secondary flow satisfies the biharmonic equation. The sequence of eddies of decreasing size and intensity first identified by Moffatt (1964*a*) is observed in each of the corners. Numerical details of a number of these eddies are given and their properties are found to be in excellent agreement with the theory.

1. Introduction

A paper by Moffatt (1964*a*) has considered in detail the structure of the two-dimensional flow of a viscous fluid in the region near a sharp corner. Moffatt studied a number of cases in which, near enough to the corner, the Stokes approximation is valid and the stream function $\psi(r, \theta)$ satisfies the biharmonic equation $\nabla^4\psi = 0$, where (r, θ) are polar co-ordinates with origin at the corner. In essence these cases merely give rise to different boundary conditions governing the flow, and the main object of the study was to show that a local solution of the biharmonic equation can be obtained which predicts that an infinite sequence of eddies of decreasing size will occur in the vicinity of the corner in all cases when the angle between the plane walls is less than a certain critical value, whose magnitude is about 146°.

The local solution of the biharmonic equation is of the form

$$\psi(r, \theta) = r^\lambda f_\lambda(\theta) \tag{1}$$

and the eddies occur only when the admissible values of λ are complex. Rayleigh (1920) showed that no solution consisting of terms of type (1) in which the admissible values of λ are integers can be found which satisfies four boundary conditions of homogeneous type, for example

$$\psi = \partial\psi/\partial\theta = 0 \quad \text{when} \quad \theta = \pm\alpha, \tag{2}$$

corresponding to zero velocity on two walls inclined at an angle 2α. Dean & Montagnon (1949) showed that λ is necessarily complex for values of 2α less than

about 146°, but it was not until the paper of Moffatt (1964*a*) that this was interpreted as implying the existence of eddies in the corner.

The solution considered by Moffatt is a similarity solution of type (1) valid only locally in the corner, and the motion in the corner must be driven in some manner. Moffatt cites several possible categories of solutions described by (1). In one of these the boundary conditions are inhomogeneous and the solutions involve positive integer values of λ. A case of this type, in which one wall moves parallel to itself with constant velocity, has been described by Taylor (1960). No eddies occur in such cases. In a second category of solutions the motion in the corner is driven by stirring of the fluid at large enough distances from the corner. Here the boundary conditions are homogeneous and of type (2). Eddies occur if α is small enough, and the real part of λ is positive. An example of this type in which the motion is driven by inhomogeneous boundary conditions at some distance from the corner has been given by Moffatt (1964*b*). A third category of solutions considered by Moffatt (1964*a*) is that in which (1) describes the flow at large distances from the corner which is driven by a disturbance near the corner. The boundary conditions are again given by (2). Eddies occur also in this case for angles in general less than about 146° but the real part of λ is negative.

In the cases considered by Moffatt (1964*a*, *b*) the governing equation is the homogeneous biharmonic equation $\nabla^4\psi = 0$. In the present paper we shall consider a somewhat different case where the flow is the two-dimensional secondary flow which occurs in the plane of a cross-section of a slightly curved tube in which the primary flow is the axial flow through the tube maintained by a constant pressure gradient. This type of problem has been the subject of many studies, but the early work was done for a tube of circular cross-section by Dean (1927, 1928). He showed that for small curvature of the tube it is possible to formulate an analysis for small perturbations from the basic Poiseuille flow when the tube is straight. The first-order perturbation for the stream function of the secondary flow satisfies an inhomogeneous biharmonic equation with a forcing term on the right-hand side due to the primary flow, which drives the secondary motion. When the cross-section contains a sharp corner, the local solution near the corner will consist of a forced term satisfying the inhomogeneous biharmonic equation together with a suitable combination of solutions of the homogeneous biharmonic equation of the type (1). If the latter terms dominate the solution, eddies may be seen.

The present investigation arose in the course of a study of flow in a curved tube whose cross-section is a right-angled isosceles triangle. The appearance of vortices was first observed in the secondary flow in the 45° corners of the cross-section and a detailed study of all the corner regions was subsequently made by refining the grid size of the numerical scheme. In this way it was possible to observe thirteen of the vortices in the 45° corner and six pairs of vortices in the 90° corner. Corner vortices of Moffatt's type have previously been observed in numerical calculations by Burggraf (1966) and by Pan & Acrivos (1967). In the latter paper a detailed study was made of three of the vortices formed in a 90° corner and their properties were found to compare favourably with the theory of Moffatt (1964*a*). The flow in the corner was in principle similar to that found in

each of the 45° corners in the present case in that it was dominated by the term of type (1) with the eigenvalue $\lambda = \lambda_1$ having the smallest possible positive real part for the appropriate angle 2α. The stream function $\psi(r, \theta)$ is symmetrical about the bisector of the corner angle in this case and the corresponding flow is antisymmetrical about this line.

In the present case, however, the flow in the 90° corner is required by the conditions of the problem to be symmetrical about the bisector of the corner angle. Thus the term of type (1) which would dominate the solution in the general case is specifically excluded and the dominant term is that with the eigenvalue $\lambda = \lambda_2$ having the smallest positive real part of all eigenvalues associated with terms for which $\psi(r, \theta)$ is antisymmetrical about the bisector. The vortices in the corner occur in symmetrical pairs in this case. Their intensity decays much more rapidly than in the general case and they are more widely separated. They can occur (Moffatt 1964*a*) for a rather wider range of angles, $2\alpha < 156°$, approximately, than that in the general case. There are no published details of calculations illustrating this case of symmetrical flow about the centre-line of a corner. The present results verify the theory for this case as far as it is possible to do so and also illustrate a case where the flow in all the corners is driven by the inhomogeneity of the biharmonic equation.

2. Equations and boundary conditions

A typical triangular cross-section of a curved tube is shown in figure 1, where C is the centre of the circle in which the tube lies. The angle at the vertex O is $2\beta = 90°$ and the cross-section is symmetrical about the axis CN, with $CO = L$ and $ON = a$. It is assumed that the ratio $a/L \ll 1$ and that the motion in the tube is maintained by a constant mean pressure gradient $\partial p'/\partial(L\phi) = -G$, where p' is the pressure and ϕ the angle which the plane of a given cross-section makes with a fixed cross-section, as shown in figure 1. The problem can be described in terms of the co-ordinate system (x', y', ϕ), where the origin is taken at the vertex O.

The equations of motion have been given by Dean (1928) under the assumption that the velocity components (u', v', w') in the directions of increase of the co-ordinates (x', y', ϕ) are independent of ϕ. If $x' = ax$, $y' = ay$ and ν is the coefficient of kinematic viscosity, we may write

$$u' = \frac{\nu \partial \psi}{a \partial y}, \quad v' = -\frac{\nu \partial \psi}{a \partial x}, \quad w' = \frac{\nu}{a}\left(\frac{2a}{L}\right)^{-\frac{1}{2}} w, \tag{3}$$

where $\psi(x, y)$ is the dimensionless stream function of the secondary flow in the cross-section. The equations of motion for $\psi(x, y)$ and $w(x, y)$ are

$$\nabla^2 w + \frac{\partial \psi}{\partial x}\frac{\partial w}{\partial y} - \frac{\partial \psi}{\partial y}\frac{\partial w}{\partial x} = -D, \tag{4}$$

$$\nabla^4 \psi + \frac{\partial \psi}{\partial x}\frac{\partial}{\partial y}(\nabla^2 \psi) - \frac{\partial \psi}{\partial y}\frac{\partial}{\partial x}(\nabla^2 \psi) + w\frac{\partial w}{\partial y} = 0, \tag{5}$$

where $$\nabla^2 = \partial^2/\partial x^2 + \partial^2/\partial y^2.$$

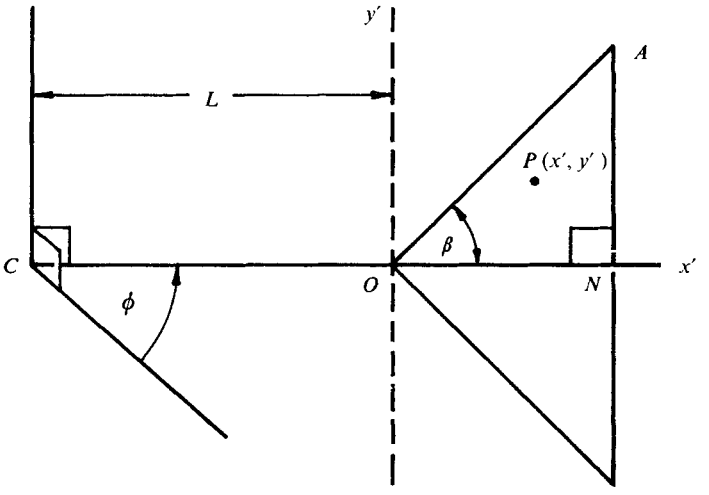

FIGURE 1. Co-ordinate system and geometry of cross-section.

The constant D is the Dean number, defined by $D = Ga^3(2a/L)^{\frac{1}{2}}/\rho\nu^2$, where ρ is the density.

If the triangular boundary in figure 1 is denoted by Δ, the boundary conditions are that

$$w = 0, \quad \partial\psi/\partial x = \partial\psi/\partial y = 0 \quad \text{on} \quad \Delta, \tag{6}$$

from which it also follows that we may take

$$\psi = 0 \quad \text{on} \quad \Delta. \tag{7}$$

In view of these conditions, if we put $D = 0$ in (4) it is found that $w(x, y) = 0$ and $\psi(x, y) = 0$ for all values of x and y within Δ. Dean (1928) showed that for small D a solution of (4) and (5) can be developed as a series in powers of D and proceeded to determine several terms in the series for a tube of circular cross-section. In the present case we shall consider only the first term of the expansion for small D by putting

$$w \sim DW(x, y), \quad \psi \sim D^2\Psi(x, y). \tag{8}$$

Then from (4) and (5) it is found that

$$\nabla^2 W + 1 = 0, \tag{9}$$

$$\nabla^4\Psi + W\partial W/\partial y = 0. \tag{10}$$

The functions W and Ψ obviously satisfy the same boundary conditions (6) and (7) as w and ψ, and numerical solutions of (9) and (10) satisfying these conditions must be found. If the solution of (9) with $W = 0$ on Δ is found and introduced into (10), the term $W\partial W/\partial y$ acts as a forcing term which drives the secondary flow. If we take local polar co-ordinates (r, θ) with origin at any of the corners of the cross-section it may be shown that the required solution of (9) has $W = O(r^2)$ as $r \to 0$ and then that the particular solution of (10) due to the forcing term $W\partial W/\partial y$ gives $\Psi = O(r^7)$ as $r \to 0$, regardless of the angle of the corner. The theory of Moffatt (1964*a*) then shows that the complete solution for

Ψ near each of the corners is dominated by the most significant term of the complementary function for Ψ, which satisfies $\nabla^4\Psi = 0$. Thus vortices may be expected in each of the corners, although the dominance of the complementary function is not great and it is necessary to obtain a very refined numerical solution, particularly near the 90° corner. It may be noted that vortices have previously been observed in other numerical investigations of flow through curved tubes, e.g. by Cheng & Akiyama (1970) and Hocking (unpublished) for a rectangular cross-section, but they do not appear to be corner vortices of Moffatt's type.

In the numerical solution of (10) it is convenient to express the problem as the pair of simultaneous equations

$$\nabla^2\Psi = -\Omega, \quad \nabla^2\Omega = W\,\partial W/\partial y. \tag{11), (12}$$

Because of the symmetry of the flow about the x axis, it is necessary to solve (9), (11) and (12) only in the upper half of the triangular region with the symmetry conditions

$$W(x,-y) = W(x,y), \quad \Psi(x,-y) = -\Psi(x,y), \quad \Omega(x,-y) = -\Omega(x,y) \tag{13a–c}$$

and, as a consequence of the last two of these conditions,

$$\Psi = \Omega = 0 \quad \text{when} \quad y = 0. \tag{14}$$

3. Numerical solutions

The equations were solved numerically by covering the triangular region with a square grid of side h, with $x = 1$ and $y = 0$ as grid lines. By suitable choice of h the grid could be made to fit exactly into the region, giving a series of uniformly spaced grid points on $y = \pm x$. Solutions were obtained over the upper half of the triangle only, making use of (13) and (14). The solution procedure is quite standard and we shall describe only certain features of it in detail. The Southwell notation for grid points is adopted (Smith 1965, p. 142), in which function values at a typical set of grid points (x_0, y_0), (x_0+h, y_0), (x_0, y_0+h), (x_0-h, y_0) and (x_0, y_0-h) are given the subscripts 0, 1, 2, 3 and 4 respectively.

Equation (9) is approximated at each typical grid point by the finite-difference equation

$$W_1+W_2+W_3+W_4-4W_0+h^2 = 0. \tag{15}$$

The solution of this set of equations is required at internal grid points with $W = 0$ on $y = x$ and $x = 1$ and with the symmetry condition $W_2 = W_4$ when (x_0, y_0) lies on $y = 0$, the latter condition corresponding to (13a).

The solution was carried out by the standard successive over-relaxation procedure and needs no further description. The same procedure was used in an overall iterative sequence to solve the sets of finite-difference equations

$$\Psi_1+\Psi_2+\Psi_3+\Psi_4-4\Psi_0+h^2\Omega_0 = 0, \tag{16}$$

$$\Omega_1+\Omega_2+\Omega_3+\Omega_4-4\Omega_0-\tfrac{1}{2}hW_0(W_2-W_4) = 0, \tag{17}$$

which were used to approximate (11) and (12) at a typical grid point. The boundary conditions for (16) are that $\Psi = 0$ on all of $y = x$, $y = 0$ and $x = 1$. For (17) the condition $\Omega = 0$ holds on $y = 0$, but it is necessary to calculate a boundary condition for Ω on both $y = x$ and $x = 1$. Here we must use the conditions for ψ given in (6), which hold equally for Ψ. Some care is necessary in this calculation in the present problem.

A standard procedure on the boundary $y = x$ would be to use the finite-difference formulae

$$2h(\partial\Psi/\partial x)_0 = \Psi_1 - \Psi_3 + O(h^3), \quad 2h(\partial\Psi/\partial y)_0 = \Psi_2 - \Psi_4 + O(h^3) \qquad (18a, b)$$

and then to replace each left side by zero and neglect the $O(h^3)$ term on each right side. The approximations thus obtained are then used to eliminate from (16) the terms Ψ_2 and Ψ_3, which are outside the triangle. Since also $\Psi_0 = 0$ on the boundary we obtain the formula

$$\Omega_0 = -2(\Psi_1 + \Psi_4)/h^2 \quad \text{on} \quad y = x, \qquad (19)$$

which may be used to calculate boundary values of Ω from internal values of Ψ. By a similar procedure using only (18a) in conjunction with (16), we obtain

$$\Omega_0 = -2\Psi_3/h^2 \quad \text{on} \quad x = 1. \qquad (20)$$

There is, however, a deficiency in accuracy in both of these approximations. The elimination of the external terms in Ψ from (16) using (18) introduces an $O(h^3)$ error into (16), whereas the general truncation error on the right sides of all of (15)–(17) is $O(h^4)$. Thus the leading error term on the right sides of (19) and (20) is $O(h)$, and whereas this may not be important in many problems it is important here in the neighbourhood of the corner vortices, where a good approximation is needed because of the rapid variation of Ψ.

The boundary approximations (19) and (20) can be improved following the method proposed by Woods (1954). The leading error terms in (18a, b) can be written as $-\frac{1}{3}h^3(\partial^3\Psi/\partial x^3)_0$ and $-\frac{1}{3}h^3(\partial^3\Psi/\partial y^3)_0$, respectively, on the right side of each equation. If we now include these terms and use the governing equation (11) and then eliminate the terms Ψ_2 and Ψ_3 from (16) we obtain the approximation

$$2\Psi_1 + 2\Psi_4 + h^2\Omega_0 + \tfrac{1}{3}h^3\left[\frac{\partial\Omega}{\partial x} - \frac{\partial\Omega}{\partial y} + \frac{\partial^2}{\partial x\partial y}\left(\frac{\partial\Psi}{\partial y} - \frac{\partial\Psi}{\partial x}\right)\right]_0 = 0,$$

in which the leading error term now consists only of the $O(h^4)$ terms already present in (16). The derivatives are now expressed in terms of suitable differences, which leads finally to the formula

$$\Omega_0 = -(2\Psi_1 + 2\Psi_4 + \Psi_8)/h^2 - \tfrac{1}{2}(\Omega_1 + \Omega_4) \quad \text{on} \quad y = x, \qquad (21)$$

where $\Psi_8 = \Psi(x_0 + h, y_0 - h)$ in terms of the Southwell notation. By means of a similar procedure on $x = 1$, making use of only (18a), we obtain

$$\Omega_0 = -3\Psi_3/h^2 - \tfrac{1}{2}\Omega_3 \quad \text{on} \quad x = 1. \qquad (22)$$

Equations (21) and (22) now both have a leading truncation error $O(h^2)$. The effect of these improved boundary approximations on the solutions was studied in detail by obtaining first approximations using (19) and (20) and then correcting

these approximate solutions using (21) and (22). The overall change in the solutions was found to be small, but significant in the region of the corner vortices.

The sets of equations (16) and (17) are each solved by the successive over-relaxation procedure at all internal points of the upper half of the triangle, with boundary conditions that are either known *a priori* or calculated from time to time from (21) and (22) in an overall sequence of iterations. The procedure is very similar to that described by Collins & Dennis (1975) in the case of flow through a curved tube of circular cross-section. As was the case in those calculations, it is necessary to introduce an averaging process for the calculation of each new set of values of Ω on the boundaries from (21) and (22). Thus for (22), for example, a new set of boundary values $\Omega_0^{(m+1)}$ is calculated from the formula

$$\Omega_0^{(m+1)} = -\omega\{3\Psi_3^{(m)}/h^2 - \tfrac{1}{2}\Omega_3^{(m)}\} + (1-\omega)\Omega_0^{(m)} \quad \text{on} \quad x = 1, \tag{23}$$

where the superscript m refers to the most recently available values of the various quantities on the right at the time the new calculation is made. The parameter ω is chosen empirically. The value $\omega = 0{\cdot}05$ was found to be satisfactory in all cases. A similar formula corresponding to (21) is available, and the same value $\omega = 0{\cdot}05$ was used.

The overall sequence of iterations for solving (16) and (17) together with the calculation of new boundary conditions from (23) and the corresponding counterpart of (21) was repeated until convergence was achieved, measured by the criterion

$$|\Omega_0^{(m+1)} - \Omega_0^{(m)}| < \epsilon \quad \text{at all boundary points,} \tag{24}$$

where ϵ is some prescribed tolerance. When (24) is satisfied it is found that the function $\Omega(x, y)$ has converged to its limiting value to the same degree of tolerance. The solution $\Psi(x, y)$ of (11) has then also converged to a suitable limit at all internal grid points. Finally, the value of the relaxation factor (see Smith 1965, pp. 149–150) used in the iterative solution of each of the sets of finite-difference equations (15)–(17) was 1·6 in every case.

4. Results

Numerical solutions were obtained over the complete upper half of the triangular region for the three grid sizes $h = \frac{1}{20}$, $\frac{1}{40}$ and $\frac{1}{80}$. The three approximations were then compared in order to estimate their approach to the true solution with decreasing grid size. It was found from this estimation that everywhere except in the local regions near the corners the approximation obtained with $h = \frac{1}{80}$ had almost certainly approached the true solution for each of the three functions W, Ψ and Ω to about four significant figures. In each of the numerical approximations the value of ϵ taken in (24) is not very relevant because the iterations were allowed to continue until each solution had approached a limit to well within the four significant figure tolerance required in estimating the approach to the true solution with decreasing h. It was found that the appearance of at least one vortex in corner A (figure 1) could be detected in each of these three solutions, but that none had thus far appeared in corner O.

The region near corner A was now magnified as follows. Since the $h = \frac{1}{80}$

solution is correct to approximately four figures on the whole of the line $y = \frac{1}{2}$, this was taken as a new boundary and a new solution was obtained with grid size $h = \frac{1}{160}$ in the triangular region between $y = \frac{1}{2}$, $y = x$ and $x = 1$. Boundary values of the three functions W, Ψ and Ω on $y = \frac{1}{2}$ were taken from the $h = \frac{1}{80}$ solution, the intermediate values necessary for the finer-grid solution being obtained by a very accurate interpolation procedure. Some check could then be obtained by comparing the $h = \frac{1}{80}$ and $h = \frac{1}{160}$ solutions, particularly at grid points far from the newly imposed boundary $y = \frac{1}{2}$. The agreement was found to be good everywhere except very near the corner at $y = 1$. Thus it was now possible to take the line $y = \frac{3}{4}$ as a new boundary and obtain a new solution with $h = \frac{1}{320}$ in the triangular region bounded by the lines $y = \frac{3}{4}$, $y = x$ and $x = 1$, using the $h = \frac{1}{160}$ solution with interpolated values to provide boundary conditions on $y = \frac{3}{4}$. This procedure of taking a new boundary parallel to the x axis and halfway between the previous boundary parallel to this direction and the line $y = 1$ was then repeated numerous times until eventually the grid size of the solution near corner A was reduced to $h = 1/41943040$. A similar method was subsequently employed to magnify the region near corner O. In this case the line $x = \frac{1}{2}$ was first taken as a boundary and a solution obtained with $h = \frac{1}{160}$ in the triangular region bounded by $y = 0$, $y = x$ and $x = \frac{1}{2}$, using the $h = \frac{1}{80}$ solution to provide boundary values on $x = \frac{1}{2}$. By following a procedure corresponding to that outlined for corner A, the grid size near corner O was eventually reduced to $h = 1/20971520$.

It is possible that in obtaining these refined solutions a more elaborate way of halving the grid size could be adopted using the graded-net technique of Allen & Dennis (1951) but this would involve substantial problems of computer storage. The above procedure seems adequate for present purposes, and to some extent a test of its adequacy lies in the satisfactory comparison found with the asymptotic theory of Moffatt (1964*a*). Thirteen of the sequence of decaying secondary vortices were identified in corner A, excluding the primary driving motion of the main secondary flow in the tube. Six of the secondary vortices, labelled $V_1, \ldots, V_6$, are shown in figure 2. Figure 2(*a*) shows the complete upper half of the cross-section with the streamlines of the main secondary flow in the tube and the position of the corner vortex V_1. Figures 2(*b*) and (*c*) show enlarged regions of the neighbourhood of corner A of the cross-section according to the scales indicated. Further diagrams could be drawn for the remaining vortices but they would add little to figure 2. The vortices clearly tend to become symmetrical about the bisector of the angle at A in accordance with theory. The same tendency was noted by Pan & Acrivos (1967) in their example. In corner O the secondary vortices consist of a sequence of vortex pairs symmetrical about the x axis. Six vortex pairs were observed in the calculations. The first four of the sequence in the region $y > 0$ are shown in figure 3 and we shall subsequently refer only to vortices in this actual region of computation. Fewer vortices were observed in corner O of this region than in corner A in the above roughly equivalent numerical investigations of each corner. The reason is that the decay of successive vortices with regard to both distance from the corner and intensity of Ψ is much more rapid near O than near A.

In order to compare some of the details of the vortices with the asymptotic theory of Moffatt (1964*a*) we shall first take local polar co-ordinates (r, θ) with origin at corner A and the initial line directed along the bisector of the 45° angle at A. Thus the boundaries $x = 1$ and $y = x$ correspond to $\theta = \pm 22{\cdot}5°$, respectively. The local solution for the stream function Ψ will in general consist of a combination of terms of the type of the right side of (1) together with an $O(r^7)$ term due to the $W\partial W/\partial y$ term in (10) and may be written as

$$\Psi = \sum_{n=1}^{\infty} A_n r^{\lambda_n} f_{\lambda_n}(\theta) + r^7 F(\theta) + o(r^7), \tag{25}$$

where the λ_n are a set of eigenvalues and the A_n are constants. The eigenfunctions $f_{\lambda_n}(\theta)$ which correspond to the eigenvalues λ_n are either even or odd functions of θ and terms of both types will generally appear in (25). In the present case the eigenvalues λ_n are complex with positive real parts, which we assume to be ordered so as to increase with increasing n. As $r \to 0$ the expansion (25) will be dominated by the term which corresponds to the eigenvalue λ_1 with the smallest real part provided $\mathrm{Re}\,\lambda_1 < 7$, and this term will then give the asymptotic nature of the flow in the corner.

The eigenfunction $f_{\lambda_1}(\theta)$ associated with λ_1 is an even function of θ, which gives antisymmetrical flow about $\theta = 0$. Unless this term is specifically excluded from (25) by imposing symmetry of the flow about $\theta = 0$, it will dominate Ψ as $r \to 0$ if $\mathrm{Re}\,\lambda_1 < 7$. It is obvious from figure 2(*c*) that the flow near A is tending to become antisymmetrical about $\theta = 0$ as $r \to 0$. For a general angle 2α the eigenvalues λ_n associated with the terms in (25) giving antisymmetrical flow about $\theta = 0$ are (Moffatt 1964*a*, p. 8)

$$\lambda_n = 1 + (2\alpha)^{-1}(\xi_n + i\eta_n), \tag{26}$$

where ξ_n and η_n are the roots of the equations

$$\sin\xi \cosh\eta = -k\xi, \quad \cos\xi \sinh\eta = -k\eta \tag{27}$$

such that

$$(2n-1)\pi < \xi_n < (2n-\tfrac{1}{2})\pi \tag{28}$$

and with $k = (\sin 2\alpha)/2\alpha$ in (27). The particular values of ξ_1 and η_1 for the case $2\alpha = 45°$ have not been given by Moffatt but are easily computed to be $\xi_1 = 4{\cdot}233$ and $\eta_1 = 2{\cdot}137$. Hence $\mathrm{Re}\,(\lambda_1) = 6{\cdot}39$ and vortices will occur in corner A. Values of ξ_1 and η_1 for the range of corner angles 2α given by Moffatt (1964*a*, p. 8) have been computed rather more accurately and are given in table 1. This table also gives values of ξ_2 and η_2, which correspond through (26) to the eigenvalue λ_2 with the smallest positive real part associated with an eigenfunction which is an odd function of θ. In the case of eigenvalues λ_n associated with $f_{\lambda_n}(\theta)$ which are odd functions of θ the roots ξ_n and η_n satisfy (27) with the minus signs suppressed and are such that

$$(2n-2)\pi < \xi_n < (2n-\tfrac{3}{2})\pi. \tag{29}$$

Finally, the present estimates of the angles $2\alpha_1$ and $2\alpha_2$ below which the eigenvalues λ_1 and λ_2, respectively, are complex are $2\alpha_1 = 146{\cdot}3°$ and $2\alpha_2 = 159{\cdot}1°$. The latter differs by a few degrees from Moffatt's value $2\alpha_2 = 156°$.

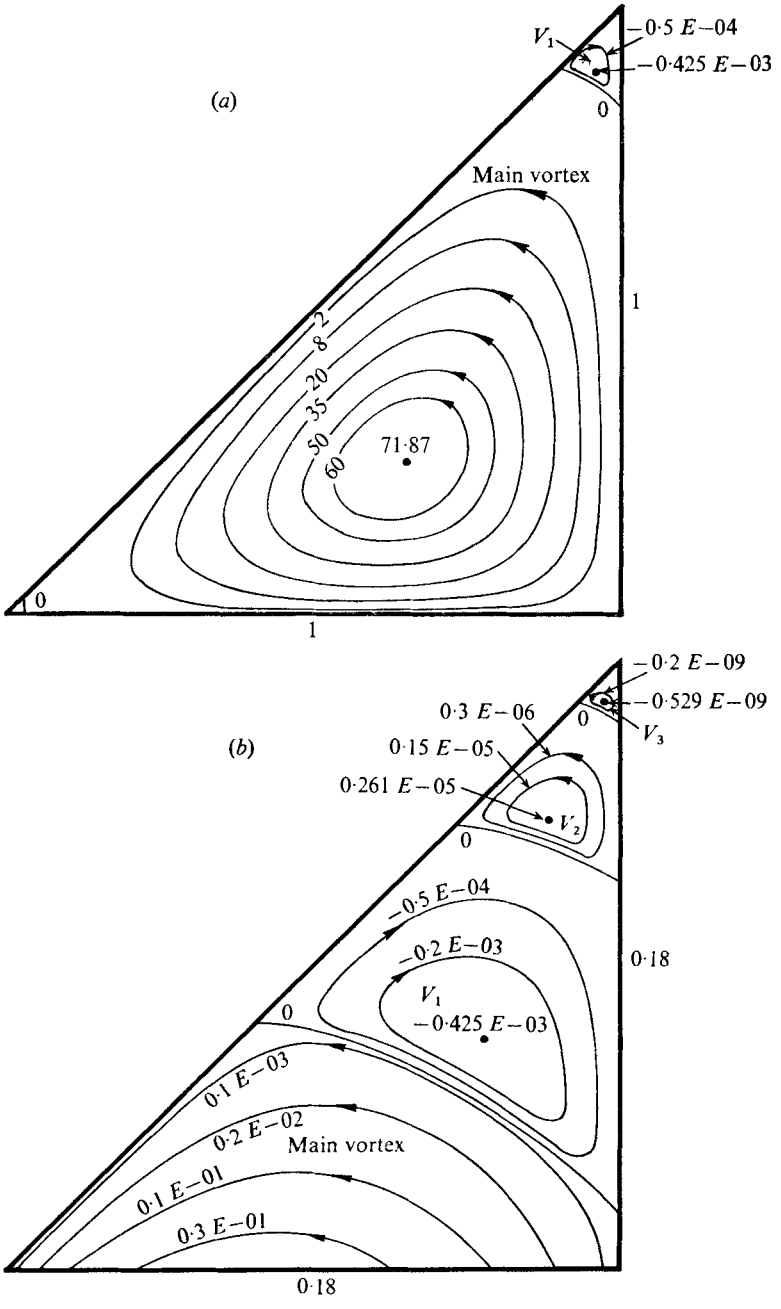

FIGURES 2 (*a*) and (*b*). For legend see facing page.

In order to consider the vortices near corner O we take local polar co-ordinates (r, θ) with origin at O and initial line along the $+x$ direction. By symmetry the sum in (25) is now composed only of terms associated with odd functions of θ and is dominated as $r \to 0$ by the term involving λ_2. Since $\alpha = \beta = \frac{1}{4}\pi$ in this case and $\xi_2 = 7{\cdot}553$ and $\eta_2 = 2{\cdot}300$ from table 1, $\mathrm{Re}\,\lambda_2 = 5{\cdot}81 < 7$ and the observation

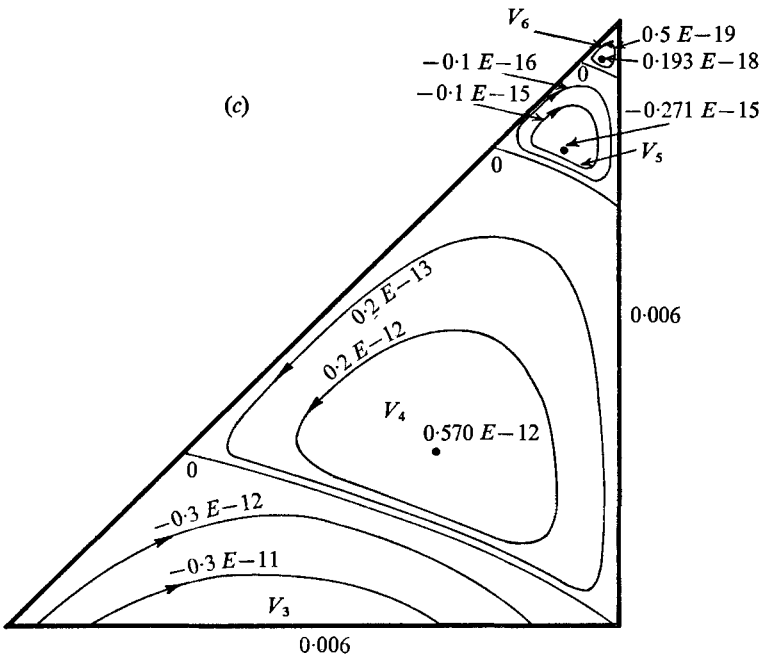

FIGURE 2. Main secondary flow and the corner vortices near corner A. (*a*) Main secondary flow and the vortex V_1. (*b*) Vortices $V_1, \ldots, V_3$. (*c*) Vortices $V_4, \ldots, V_6$. The value of Ψ' at the centre of each corner vortex is given in table 2. Values of Ψ' are given on the streamlines.

of vortices in the corner is consistent with theory. We shall now make some brief comparisons of calculated properties of the vortices with Moffatt's theory in both corner O and corner A. It is convenient to consider both cases together, having due regard for the significance of the co-ordinates (r, θ) in each case. The asymptotic expression for Ψ' as $r \to 0$ can be written from Moffatt's theory as

$$\Psi' \sim \mathrm{Re}\,[(B+iC)\, r^{\lambda} f_{\lambda}(\theta)], \tag{30}$$

where

$$\lambda = \lambda_1, \quad f_{\lambda_1}(\theta) = \cos\lambda_1\theta \cos\tfrac{1}{8}(\lambda_1 - 2)\pi - \cos(\lambda_1 - 2)\theta \cos\tfrac{1}{8}\lambda_1\pi$$

near corner A and

$$\lambda = \lambda_2, \quad f_{\lambda_2}(\theta) = \sin\lambda_2\theta \sin\tfrac{1}{4}(\lambda_2 - 2)\pi - \sin(\lambda_2 - 2)\theta \sin\tfrac{1}{4}\lambda_2\pi$$

near corner O. The complex constant $B+iC$ can only be determined from a knowledge of the specific flow in the corner or, in principle, from the conditions specifying it.

The centre of a particular vortex may be defined as a point of zero velocity, i.e. a local maximum or minimum of Ψ'. For the asymptotic expression (30) the centres of the vortices all lie on $\theta = 0$ for the case $\lambda = \lambda_1$, but for the case $\lambda = \lambda_2$ it is not in general possible to determine the angle $\theta = \theta_c$ which the line joining the centre of a given vortex to the corner makes with the initial line $\theta = 0$. In the present case of the flow near corner O it will be verified below that θ_c tends to become constant as $r \to 0$ and that this is consistent with (30) for the case $\lambda = \lambda_2$.

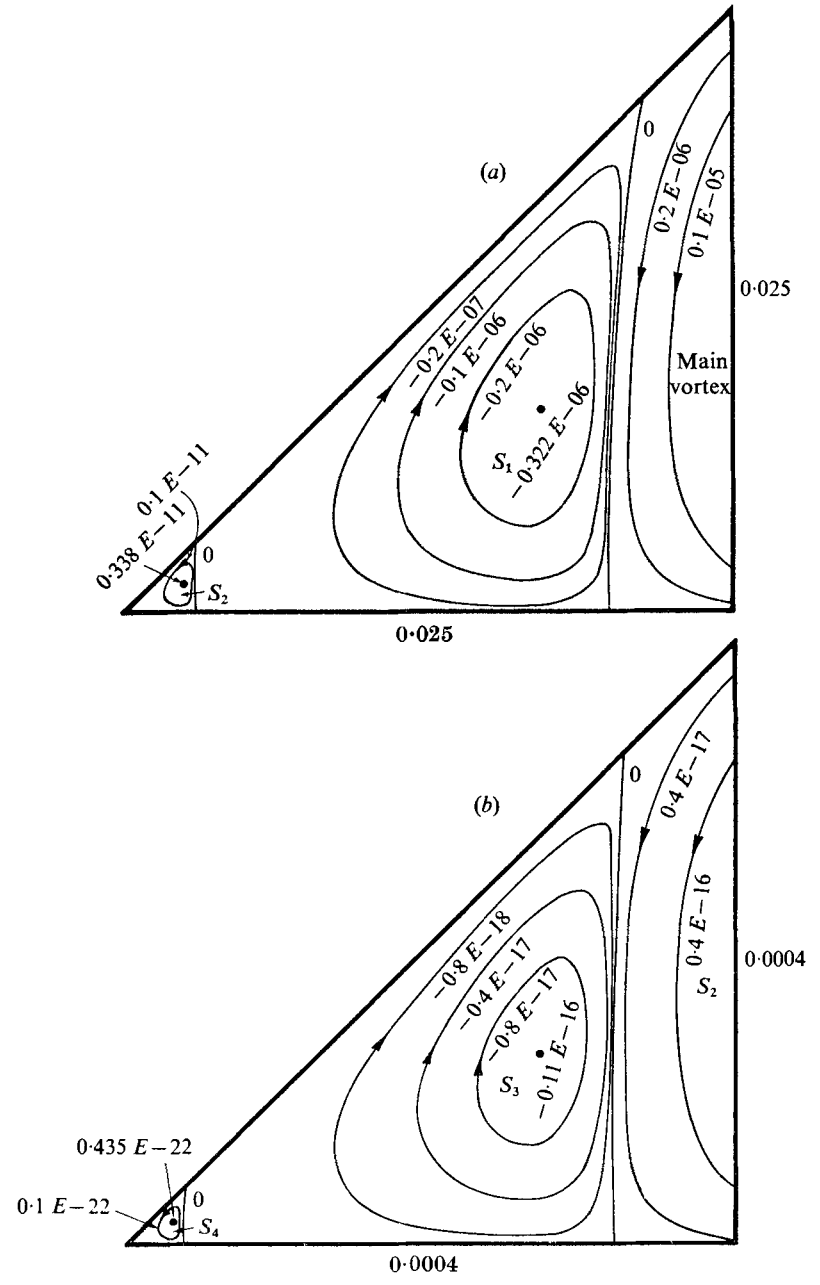

FIGURE 3. Corner vortices in the region $\theta > 0$ near corner O. (*a*) Vortices S_1 and S_2. (*b*) Vortices S_3 and S_4. The value of Ψ at the centre of each corner vortex is given in table 3. Values of Ψ are given on the streamlines.

We can then obtain two theoretical properties of the centres from (30) to compare with the numerical results. Both can be readily obtained from the results given by Moffatt (1964*a*). The first gives the ratio of the positions of the centres of the vortices in the form

$$r_n/r_{n+1} = \exp(2\alpha\pi/\eta), \tag{31}$$

2α (deg)	ξ_1	η_1	ξ_2	η_2
0	4·212	2·251	7·498	2·769
10	4·213	2·245	7·498	2·763
20	4·217	2·229	7·500	2·748
30	4·222	2·201	7·503	2·721
40	4·229	2·161	7·508	2·683
50	4·239	2·109	7·514	2·633
60	4·251	2·044	7·521	2·572
70	4·266	1·965	7·530	2·496
80	4·283	1·870	7·540	2·406
90	4·303	1·758	7·553	2·300
100	4·327	1·624	7·567	2·174
110	4·354	1·463	7·584	2·024
120	4·386	1·266	7·604	1·846
130	4·422	1·013	7·627	1·627
140	4·464	0·639	7·655	1·348
$2\alpha_1$	4·493	0·000	—	—
150	—	—	7·688	0·952
$2\alpha_2$	—	—	7·725	0·000

TABLE 1. Values of ξ_n and η_n for various corner angles 2α. The critical angles below which λ_1 and λ_2 are complex are $2\alpha_1 = 146{\cdot}3°$ and $2\alpha_2 = 159{\cdot}1°$, respectively.

where r_n is the distance of the centre of the nth vortex (V_n in figure 2 and S_n in figure 3) from the respective corner and $\eta = \eta_1$ when $\lambda = \lambda_1$ and $\eta = \eta_2$ when $\lambda = \lambda_2$. The second gives the ratio $\Psi_{r_n}/\Psi_{r_{n+1}}$ of the stream function at the centres of successive vortices. The modulus of the reciprocal of this quantity gives a measure of the decay of the absolute intensity of the stream function in the successive vortices as the corner is approached. It is easily shown that

$$\Psi_{r_n}/\Psi_{r_{n+1}} = -(r_n/r_{n+1})^{\xi/2\alpha+1}.$$

Hence if M_n denotes the modulus of the ratio on the left side, we obtain from (31)

$$M_n = \exp[\pi(\xi + 2\alpha)/\eta], \tag{32}$$

where ξ and η must be taken as the values corresponding to λ_1 and λ_2 in the respective cases.

Moffatt gives a somewhat more realistic measure of the decay of intensity of consecutive vortices for the case of antisymmetrical flow about $\theta = 0$ by calculating the ratio of the greatest velocity on $\theta = 0$ for each of two successive vortices. However, this property is more difficult to calculate from the present numerical solutions and (32) will be used instead. As it is, we have to find the positions of the local maxima and minima of Ψ by an interpolation procedure. The process used for the interpolation is briefly described since it helps to give some notion of the accuracy to be expected in the subsequent comparisons. Within a given vortex the point observed to have the locally greatest absolute value of Ψ is first located. If this is the point (x_0, y_0) with an associated value Ψ_0 we may then approximate $\Psi(x, y)$ in its neighbourhood in the form

$$\Psi \sim \Psi_0 + aX + bY + cX^2 + 2dXY + eY^2 + \ldots, \tag{33}$$

Vortex	n	θ_c (deg)	r_n	r_n/r_{n+1}	Ψ_c	M_n
V_1	1	3·02	$0{\cdot}1192E+00$	2·327	$-0{\cdot}4251E-03$	163
V_2	2	−1·17	$0{\cdot}5123E-01$	3·761	$0{\cdot}2614E-05$	4940
V_3	3	0·57	$0{\cdot}1362E-01$	2·936	$-0{\cdot}5292E-09$	929
V_4	4	−0·32	$0{\cdot}4638E-02$	3·300	$0{\cdot}5698E-12$	2104
V_5	5	0·14	$0{\cdot}1405E-02$	3·115	$-0{\cdot}2708E-15$	1403
V_6	6	−0·11	$0{\cdot}4512E-03$	3·204	$0{\cdot}1930E-18$	1714
V_7	7	−0·01	$0{\cdot}1408E-03$	3·157	$-0{\cdot}1126E-21$	1553
V_8	8	−0·04	$0{\cdot}4459E-04$	3·181	$0{\cdot}7250E-25$	1630
V_9	9	−0·01	$0{\cdot}1402E-04$	3·171	$-0{\cdot}4447E-28$	1592
V_{10}	10	−0·04	$0{\cdot}4422E-05$	3·175	$0{\cdot}2794E-31$	1611

TABLE 2. Properties of the vortices near the 45° corners calculated from the numerical solutions. The theoretical limits of r_n/r_{n+1} and M_n as $n \to \infty$ are 3·173 and 1600 respectively.

where $X = x - x_0$, $Y = y - y_0$ and terms above the second degree in X and Y are neglected. We now put $\partial\Psi/\partial X = 0$ and $\partial\Psi/\partial Y = 0$ in (33), which gives two linear equations in X and Y whose solution gives an approximation to the position of the local maximum or minimum of Ψ. Substitution of this approximation in (33) gives the maximum or minimum Ψ. The constants in (33) can all be expressed in terms of the appropriate derivatives of Ψ at (x_0, y_0) and these in turn may be approximated by central-difference formulae in terms of Ψ_0 and the values of Ψ at the eight points of the grid on the square surrounding (x_0, y_0). Thus, for example,

$$2d = (\partial^2\Psi/\partial x\,\partial y)_0 \simeq (\Psi_5 - \Psi_6 + \Psi_7 - \Psi_8)/4h^2$$

in terms of the Southwell notation, and the formulae for the other derivatives involved are quite well known.

The results of the calculations for corner A are shown in table 2. Details are given for only ten of the vortices since, although thirteen were observed, the amount of numerical detail becomes less as the corner is approached. Two of the columns of figures give the estimated polar co-ordinates of the centres relative to A with the internal bisector of the angle at A as the initial line $\theta = 0$. Two further columns give numerical estimates which can be compared with the theoretical estimates as $r \to 0$ given by (31) and (32). The floating-point notation for decimal numbers is used where it is more convenient to do so. The theoretical estimate of the limit of r_n/r_{n+1} given by (31) is easily calculated to be $r_n/r_{n+1} = 3{\cdot}173$ and the theoretical result for M_n from (32) is $M_n = 1600$. Within the limits of numerical error, therefore, and bearing particularly in mind that all the results quoted in table 2 were obtained by interpolation, the agreement with the asymptotic theory is good. It is true that the tendency $\theta_c \to 0$ as $r \to 0$ is not exceptionally well delineated by the results on a fine scale, but even so the results are satisfactory enough, measured as a percentage of the 45° corner angle.

The corresponding results for four of the computed vortices in the region $\theta > 0$ near corner O are shown in table 3. Here the scale of decay of the vortices

Vortex	n	θ_c (deg)	r_n	r_n/r_{n+1}	Ψ_{r_n}	$M_n \times 10^{-5}$
S_1	1	25·76	$0{\cdot}1908E-01$	7·209	$-0{\cdot}3219E-06$	0 954
S_2	2	24·74	$0{\cdot}2646E-02$	8·813	$0{\cdot}3376E-11$	3·069
S_3	3	24·94	$0{\cdot}3002E-03$	8·519	$-0{\cdot}1100E-16$	2·529
S_4	4	24·91	$0{\cdot}3524E-04$	8·547	$0{\cdot}4349E-22$	2·592

TABLE 3. Properties of the symmetrical vortex pairs near the 90° corner calculated from the numerical solutions. The theoretical limits of r_n/r_{n+1} and $M_n \times 10^{-5}$ as $n \to \infty$ are 8·547 and 2·584 respectively.

as $r \to 0$ is very much greater and the theoretical limits obtained from (31) and (32) correspond to $r_n/r_{n+1} = 8{\cdot}547$ and $M_n \times 10^{-5} = 2{\cdot}584$, which show good agreement with the numerical results. The angle θ_c appears to have approached close to a limit by the time the fourth vortex is reached and this was checked with Moffatt's theory in the following way. The expression (30) for Ψ was evaluated by using the known real and imaginary parts of $f_{\lambda_2}(\theta)$ when $\lambda = \lambda_2$ and the constants B and C found by fitting the resulting expression to the computed Ψ in the fifth of the observed vortices. This was done for a range of values of θ, each time finding A and B by fitting (30) to values of Ψ at two distinct values of r sufficiently far from the corner for the computed solution to be accurate. The result of the many fits was to give the same consistent values $B = -2602$ and $C = -6837$ and the expression (30) was then found to agree with the computed Ψ in the fifth vortex everywhere except very close to the corner. The expression (30) was then used to calculate the theoretical positions of the centres of the sixth and a number of subsequent vortices and these were all found to yield $\theta_c = 24{\cdot}916°$. These combined tests of the theory would seem to give an adequate check in the present case and presumably other properties could be checked satisfactorily.

The present work arose in an investigation of flow through a curved tube of triangular cross-section which was stimulated by a theoretical paper by Dr F. T. Smith (1976) and by discussions with Professor N. Riley. The authors are greatly indebted to comments by a referee on a previous version of this paper. The investigation has been supported by a grant from the National Research Council of Canada.

REFERENCES

ALLEN, D. N. DE G. & DENNIS, S. C. R. 1951 *Quart. J. Mech. Appl. Math.* **4**, 439.
BURGGRAF, O. R. 1966 *J. Fluid Mech.* **24**, 113.
CHENG, K. C. & AKIYAMA, M. 1970 *Int. J. Heat Mass Transfer*, **13**, 471.
COLLINS, W. M. & DENNIS, S. C. R. 1975 *Quart. J. Mech. Appl. Math.* **28**, 133.
DEAN, W. R. 1927 *Phil. Mag.* **4**, 208.
DEAN, W. R. 1928 *Phil. Mag.* **5**, 673.
DEAN, W. R. & MONTAGNON, P. E. 1949 *Proc. Camb. Phil. Soc.* **45**, 389.
MOFFATT, H. K. 1964*a* *J. Fluid Mech.* **18**, 1.
MOFFATT, H. K. 1964*b* *Arch. Mech. Stosowanej*, **14**, 365.

PAN, F. & ACRIVOS, A. 1967 *J. Fluid Mech.* **28**, 643.

RAYLEIGH, LORD 1920 *Scientific Papers*, vol. 6, p. 18. Cambridge University Press.

SMITH, F. T. 1976 *Proc. Roy. Soc.* A **347**, 345.

SMITH, G. D. 1965 *Numerical Solution of Partial Differential Equations*. Oxford University Press.

TAYLOR, G. I. 1960 *Aeronautics and Astronautics* (ed. Hoff & Vincenti), p. 12. Pergamon.

WOODS, L. C. 1954 *Aero. Quart.* **5**, 176.